FINITE ELEMENT ANALYSIS OF COMPOSITE BALLISTIC HELMET SUBJECTED TO HIGH VELOCITY IMPACT

ROZAINI BIN OTHMAN

UNIVERSITI SAINS MALAYSIA

2009

FINITE ELEMENT ANALYSIS OF COMPOSITE BALLISTIC HELMET SUBJECTED TO HIGH VELOCITY IMPACT

by

ROZAINI BIN OTHMAN

Thesis submitted in fulfillment of the requirements
for the degree of
Master of Science

March 2009

ACKNOWLEDGEMENTS

In The Name of Allah, The Most Gracious and The Most Merciful

First and foremost, I would like to express my sincere gratitude and highest appreciation to my supervisor Assoc. Prof. Dr Roslan Ahmad for his valuable guidance, support, advice and encouragement throughout my Master of Science study. My special acknowledgement is dedicated to Universiti Teknologi MARA for providing me the scholarship through the Young Lecturer Scheme during my period of study. I also would like to thank Mr. Salleh Omar from AMREC-SIRIM for providing ballistic helmet model that has been used in this work.

Apart from that, I would like to express my gratefulness to my beloved family for their support especially to my parents who have done the most excellent in providing me with the education. To my beloved wife, Zaiton Binti Din, there is nothing more I could say except thank you for the patience, moral support and encouragement throughout my academic journey as well as taking a good care of our first child, Ammar As-Syatir. I also would like to acknowledge my entire friends for their great and favourable support. Last but not least, a truly thankfulness is dedicated to all who has helped and supported me in one way or another. Thank you very much and may Allah grant all of you with His mercy and reward.

ROZAINI BIN OTHMAN

March 2009.

TABLE OF CONTENTS

Acknowledgements ii

Table of Contents iii

List of Tables vii

List of Figures viii

List of Symbols xi

Abbreviations xiii

Abstrak xiv

Abstract xvi

CHAPTER 1 - INTRODUCTION

1.0 Background 1

1.1 Problem Identification 5

1.2 Scope of Research 5

1.3 Objective of Research 6

1.4 Thesis Outline 6

CHAPTER 2 – LITERATURE REVIEW

2.0 Introduction 8

2.1 Constitutive Modelling 9

2.1.1 Composite Materials 9

2.1.1.1 Orthotropic Material 11

2.1.2 Impact Dynamics 14

2.1.2.1 Fundamental Principle 14

2.2 Penetration Mechanisms of Composite Materials 15

2.3 Energy Absorption Mechanisms of Composite Materials 19
2.4 Numerical Modelling of Ballistic Impact 21
2.5 Parameters Affecting Ballistic Performance 23
2.5.1 Material Properties 23
2.5.2 Effect of Projectile Geometry 26
2.5.3 Effect of Thickness 30
2.5.4 Effect of Impact Velocity 33
2.6 Ballistic Helmet 35
2.6.1 Ballistic Helmet Test Standard 35
2.6.2 Ballistic Helmet Design 36
2.6.2.1 Ballistic Resistance 36
2.6.2.2 Material Consideration and Manufacturing Technique 38
2.6.2.3 Weight 39
2.6.2.4 Balance 39
2.6.2.5 Helmet-to-Person Interface 40
2.6.3 Biomechanical Impact of Ballistic Helmet 40
2.7 Discussion 42
2.8 Summary 43

CHAPTER 3 – METHODOLOGY OF RESEARCH

3.0 Introduction 45
3.1 Finite Element Modelling 47
3.1.1 Ballistic Helmet 47
3.1.1.1 Material Properties 49
3.1.2 Projectile 52

3.1.3 Step 53
3.1.4 Interaction 53
3.1.5 Boundary Conditions 54
3.2 Verification 54
3.3 Ballistic Limit 55
3.4 Summary 55

CHAPTER 4 – RESULTS AND DISCUSSION

4.0 Introduction 56
4.1 Verification of Finite Element Model 57
4.1.1 Choice of Mesh 60
4.2 Parametric Study 61
4.2.1 Effect of Young's Modulus 61
4.2.1.1 In-plane and Out-of-plane Young's Modulus 61
4.2.1.2 Combination of in-plane and out-of-plane Young's Modulus 62
4.2.2 Effect of Modulus of Rigidity 63
4.3 Deformation of Ballistic Helmet 64
4.4 Energy Distribution 70
4.5 Ballistic Limit 73
4.6 Residual Velocity 75
4.7 Failure Mechanisms at Ballistic Limit 77
4.8 Discussion 81
4.9 Limitation of The Model 83

CHAPTER 5 – CONCLUSION

5.0 Conclusion 85

5.1 Recommendations for Future Work 86

BIBLIOGRAPHY 87

APPENDICES 91

LIST OF PUBLICATIONS 95

LIST OF TABLES

Page

Table 2.1	Test standard of NIJ-STD-0106.01	**35**
Table 3.1	Material properties of woven Kevlar 29/Phenolic	**52**
Table 4.1	Comparison of helmet deflection based on the results obtained from ABAQUS/Explicit, LS-DYNA and experiment	**58**
Table 4.2	Ballistic limit of the helmet for each composite material	**74**
Table 4.3	Comparison of ballistic limit for Kevlar 29/Phenolic	**83**

LIST OF FIGURES

		Page
Figure 1.1	Historical perspective of U.S. Army helmet design and materials	**1**
Figure 1.2	PASGT helmet	**2**
Figure 2.1	Principal material directions in an orthotropic material	**12**
Figure 2.2	Penetration damage mechanisms in chronological order occurred during penetration process	**16**
Figure 2.3	Conical formation at the back of the panel	**17**
Figure 2.4	Damage mechanisms occurred in composite materials under ballistic impact	**17**
Figure 2.5	Damage characteristic of (a) thin target and (b) thick target. Impact face is the upper edge	**18**
Figure 2.6	Petaling	**25**
Figure 2.7	Bulging	**25**
Figure 2.8	Various shape of projectiles	**27**
Figure 2.9	The penetration of fragment simulating projectile that creates small shear zone and followed by elastic/plastic hole enlargement	**28**
Figure 2.10	Comparison of the theoretical predictions (—) and the experiment (O)for the perforation of E-glass/Polyester laminates struck by 17.9 g 10.5 mm diameter hemispherical-ended projectile	**29**
Figure 2.11	Ballistic limits versus laminate thickness and prediction for: a) Kevlar 29/Polyester laminates impacted by a projectile with diameter 12.7 mm and 9.525 respectively; b) Carbon/Epoxy laminates impacted by a projectile with diameter 2.7 mm	**30**
Figure 2.12	Kinetic energy vs target thickness for four types of projectile. The projectiles are 6.35 mm and 4.76 mm diameter flat ended-projectiles respectively and 4.76 mm diameter 90^o and 45^o conically nosed-projectiles respectively. The dashed line is the predicted curve for 6.35 mm diameter flat ended-projectile	**31**
Figure 2.13	The variation of the speed of elasticity with the number of composite plates for six different projectiles	**32**
Figure 2.14	The relationship of speed with the depth of trace for: (1) 22 layers, (2) 28 layers and (3) 36 layers	**32**

Figure 2.15	Back face damage of 6.5 mm thick target with different projectiles: (A) fragment simulating, (B) hemispherical, (C) conical, (D) flat	**33**
Figure 3.1	Flow chart of overall research methodology	**46**
Figure 3.2	(a) Dimensions of ballistic helmet model; (b) the actual ballistic helmet used by military army	**48**
Figure 3.3	Finite element mesh of the ballistic helmet	**49**
Figure 3.4	Dimension of the bullet used in the simulation	**53**
Figure 3.5	Boundary conditions implemented on bullet and ballistic helmet	**54**
Figure 4.1	Deflection of the helmet at node 174	**57**
Figure 4.2	Backplane deflection of Kevlar flat panel impacted by 1.1 g FSP at 586 m/s	**58**
Figure 4.3	History of impact velocity at duration of 200 μs	**59**
Figure 4.4	History of impact velocities	**59**
Figure 4.5	Maximum deflection occurred inside the helmet with different number of elements. (a) in-plane (b) through thickness	**60**
Figure 4.6	Number of elements at the impacted area. (a) in-plane (b) through thickness	**60**
Figure 4.7	The effect of in-plane and out-of-plane stiffness on the deflection of ballistic helmet	**62**
Figure 4.8	The effect of combination of both in-plane and out-of-plane stiffness on the deflection of ballistic helmet	**63**
Figure 4.9	The effect of in-plane and out-of-plane modulus of rigidity on the deflection of ballistic helmet	**64**
Figure 4.10	The graph of deflection vs time occurred at node 174	**64**
Figure 4.11	The deformation contour of ballistic helmet made of Carbon/Polyester when impacted at 360 m/s	**66**
Figure 4.12	The deformation contour of ballistic helmet made of Glass/Polyester when impacted at 360 m/s	**67**
Figure 4.13	The deformation contour of ballistic helmet made of Kevlar/Polyester when impacted at 360 m/s	**68**

Figure 4.14	The deformation contour of ballistic helmet made of Kevlar 29/Phenolic when impacted at 360 m/s	**69**
Figure 4.15	High-speed photograph of the back face of an aramid composite upon impact by steel sphere	**70**
Figure 4.16	The graph of kinetic energy distribution of the bullet	**71**
Figure 4.17	The graph of strain energy vs time of the ballistic helmet	**72**
Figure 4.18	The graph of total energy vs time of the ballistic helmet	**73**
Figure 4.19	The history of bullet velocity at ballistic limit for different type of fibre reinforced composites	75
Figure 4.20	Bullet starts to penetrate the ballistic helmet made of Kevlar 29/Phenolic at time t = 30 μs under impact velocity of 575.7 m/s	**75**
Figure 4.21	The relationship of residual and impact velocity for four types of composite	**76**
Figure 4.22	The variation of stress in *z*-axis for four different types of composite materials	**78**
Figure 4.23	Conical formation at the interior of the helmet at V_{50}. a) Carbon/Polyester, b) Glass/Polyester c) Kevlar/Polyester d) Kevlar 29/Phenolic	**79**
Figure 4.24	The variation of maximum principal strain for four different types of composite materials	**80**
Figure 4.25	Straining of the fibres upon impacted at V_{50}. a) Carbon/Polyester, b) Glass/Polyester c) Kevlar/Polyester d) Kevlar 29/Phenolic	**80**
Figure 4.26	The variation of in-plane shear stress for four different types of composite materials	**81**

LIST OF SYMBOLS

$\boldsymbol{C}$	material stiffness matrix
E	strain energy
E_{D}	energy absorbed by deformation of secondary yarns
E_{dl}	delamination energy
E_{DL}	energy absorbed by delamination
E_{DP}	dynamic penetration energy
E_{f}	energy absorbed during perforation due to friction
E_{F}	energy absorbed by friction
E_{ij}	Young's Modulus
E_{KE}	kinetic energy of moving cone
E_{MC}	energy absorbed by matrix cracking
E_{sh}	energy absorbed locally due to shear
E_{SP}	energy absorbed by shear plugging
E_{TF}	energy absorbed by tensile failure of primary yarns
F	force
G_{ij}	shear modulus or modulus of rigidity
$\boldsymbol{K}$	stiffness matrix
m	mass
m_p	mass of projectile
$\boldsymbol{M}$	mass matrix
S_{ij}	strength
t	time
u	displacement

$\dot{u}$	velocity
$\ddot{u}$	acceleration
V	volume
V_{50}	ballistic limit
W	work
σ	stress
ε	strain
ρ	density
τ	shear stress
Δt	the increment of time
v_{ij}	poissons ratio
υ	velocity
υ_{impact}	impact velocity
$\upsilon_{residual}$	residual velocity
γ	shear strain

ABBREVIATION

PASGT	personnel armour system ground troops
FSP	fragment simulating projectile
FRP	fibre reinforced polymer
CMM	coordinate measuring machine
CAD	computer aided design

ANALISIS UNSUR TERHINGGA KE ATAS HELMET BALISTIK KOMPOSIT YANG DIKENAKAN HENTAMAN HALAJU TINGGI

ABSTRAK

Helmet balistik yang diperbuat daripada bahan komposit telah menjadi helmet yang lebih baik daripada helmet balistik tradisional yang diperbuat daripada keluli dari aspek pengurangan berat dan peningkatan rintangan balistik. Namun begitu, tindak balas bahan komposit terhadap hentaman halaju tinggi adalah kompleks dan data yang diperolehi daripada ujian balistik adalah terhad. Ini menjadikan eksperimen untuk mengkaji ciri helmet balistik adalah mahal dan mengambil masa yang lama. Oleh itu, kaedah analisis unsur terhingga boleh digunakan sebagai kaedah untuk mengkaji tindak balas helmet balistik komposit dan memperolehi maklumat berkaitan parameter yang boleh mempengaruhi keadaan hentaman. Objektif kajian ini adalah untuk menentukan kesan modulus elastik dan modulus ricihan bahan komposit terhadap rintangan balistik. Selanjutnya, had balistik helmet yang diperbuat daripada empat jenis bahan komposit iaitu Poliester Tertulang Gentian Karbon, Poliester Tertulang Gentian Kaca, Poliester Tertulang Kevlar dan Fenolik Tertulang Kevlar 29 adalah ditentukan berserta mekanisme kegagalan yang berlaku pada helmet balistik. Selain daripada itu, ubahbentuk dan pengagihan tenaga helmet balistik apabila dihentam oleh peluru pada halaju 360 m/s akan dianalisa. Halaju hentaman adalah di antara 360 m/s hingga had balistik bagi setiap bahan komposit yang dikaji. Jenis helmet balistik yang digunakan adalah PASGT *(Personnel Armour System Ground Troops)* dengan berat 1.45 kg dan ketebalan 8mm. Helmet balistik dimodelkan adalah sebagai jasad pepejal bolehubah bentuk *(deformable solid body)* Sementara itu, jenis peluru yang digunakan adalah

peluru 9 mm parabellum dan dimodelkan sebagai jasad tegar *(rigid body).* Pengesahan model dilakukan secara perbandingan dengan data keputusan yang telah diterbitkan dan didapati hubung kait yang baik telah diperhatikan. Daripada simulasi, nilai had balistik bagi helmet balistik yang diperbuat daripada Karbon/Poliester adalah 776.8 m/s, Kaca/Poliester adalah 745.3 m/s, Kevlar/Poliester adalah 657 m/s dan Kevlar 29/Fenolik adalah 575.7 m/s. Manakala, anjakan Kevlar 29/Fenolik pula didapati adalah tertinggi apabila dikenakan hentaman pada halaju 360 m/s. Mekanisme kegagalan helmet balistik menunjukkan ia bermula dengan penghacuran matriks apabila bahan yang berada di hadapan peluru dimampatkan. Kemudian, ia diikuti pula dengan terikan dan ricihan gentian. Hasil keputusan yang diperolehi, didapati analisis unsur terhingga mampu untuk meramalkan tindak balas helmet balistik yang dikenakan hentaman pada halaju tinggi.

FINITE ELEMENT ANALYSIS OF COMPOSITE BALLISTIC HELMET SUBJECTED TO HIGH VELOCITY IMPACT

ABSTRACT

Ballistic helmet made of composite materials has become a better helmet compared to traditional steel helmet in terms of its reduction in weight and an improvement in ballistic resistance. However, the complex response of composite materials coupled with high costs and limited amount of data from ballistic testing has lead to experimental characterisation of ballistic helmet becomes expensive and time consuming. Therefore, finite element analysis can be used as a method to characterise the response of composite ballistic helmet and to obtain valuable information on parameters affecting impact phenomena. The objective of this study is to determine the effect of modulus of elasticity and shear modulus of composite materials on ballistic resistance. Apart from that, the deformation and energy distribution of the helmet when struck by a bullet at velocity of 360m/s will be analysed. In addition, the ballistic limit of the helmet made of four different types of composites namely Carbon fibre-reinforced Polyester, Glass fibre-reinforced Polyester, Kevlar fibre-reinforced Polyester and Kevlar 29 fibre-reinforced Phenolic are to be determined as well as failure mechanism occurred on the ballistic helmet. The impact velocity varied from 360 m/s to the ballistic limit for each composite material investigated. The ballistic helmet used was from type of PASGT (Personnel Armour System Ground Troops) with weight 1.45 kg and shell thickness of 8mm. The helmet was modelled as a deformable solid body. On the other hand, the bullet used was 9 mm parabellum bullet and it was modelled as a rigid body. The model was validated against published data and good correlation was observed. From the

simulation, it was determined that the ballistic limit of the helmet made of Carbon/Polyester was 776.8 m/s, Glass/Polyester was 745.3 m/s, Kevlar/Polyester was 657 m/s and Kevlar 29/Phenolic was 575.7 m/s. On the other hand, the deflection of Kevlar 29/Phenolic was found to be the highest when impacted at 360 m/s. The failure mechanism of ballistic helmet started with a matrix crushing as the material ahead of bullet being compressed. Then, it followed by straining and shearing of the fibres. From the results obtained, it was found that finite element analysis is capable of predicting the response of ballistic helmet subjected to high velocity impact.

CHAPTER 1
INTRODUCTION

1.0 Background

Helmet has been used as protective equipment in order to shield human head from impact-induced injuries such as in traffic accident, sports, construction work, military, factory and some other human activities. Typical applications of the helmet are for motorcyclists, bicycle riders, soldiers, boxers and ice hockey players. The helmets attempt to guard the wearer's head through mechanical energy absorbing process. Hence, the structure and protective capacity of the helmets are altered in high energy impact.

The head and neck represent 12% of the body area typically exposed in the battle field yet receive up to 25% of all "hits" because the soldier must continually survey his surroundings. In addition, almost half of all combat deaths are due to head injuries. Thus, it is crucial to have ballistic helmet designed in such a way that will protect the soldier's head from injury. As such, the helmet materials and designs have been improved from time to time mainly in the presence of prevailing threats and the invention of new and improved ballistic materials. Figure 1.1 shows the evolution of U.S helmet designs and materials since World War I.

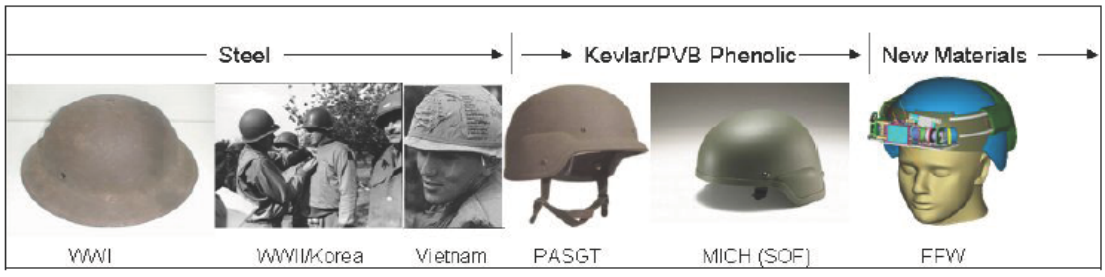

Figure 1.1: Historical perspective of U.S. Army helmet design and materials (Walsh et al., 2005)

Historically, the helmet used by the soldiers was reintroduced during World War I by General Adrian of the French army. General Adrian had made 700,000 metal caps (calotte) and were able to defeat 60% of the metal-fragment hits and saved his soldiers from severe head wound (Carey et al., 2000).

The development of the army helmet was continued with the introduction of M-1 helmet by the American troops during the outbreak of World War II, Korean War and Vietnam War. It consists of steel outer shell and inner liner shell made of cotton fabric-reinforced phenolic laminate. (Walsh et al., 2005).

The PASGT was fielded in 1982 and first used in Grenada 1983. The shell was made of Kevlar 29 fibres reinforced with resin and moulded under heat and pressure. The helmet came with five sizes and weight in the range of 1.31 kg to 1.9 kg. The bulge ear section was to provide the space for communications equipment. The retention-suspension system, fixed on the shell, was made of nylon webbing in the form of basket to provide a stable helmet-head interface. The standoff distance between the head and the helmet was 12.3mm, thus it allowed for ventilation and heat transfer as well as transient deformation due to ballistic impact (Carey et al., 2000). Figure 1.2 shows the PASGT helmet.

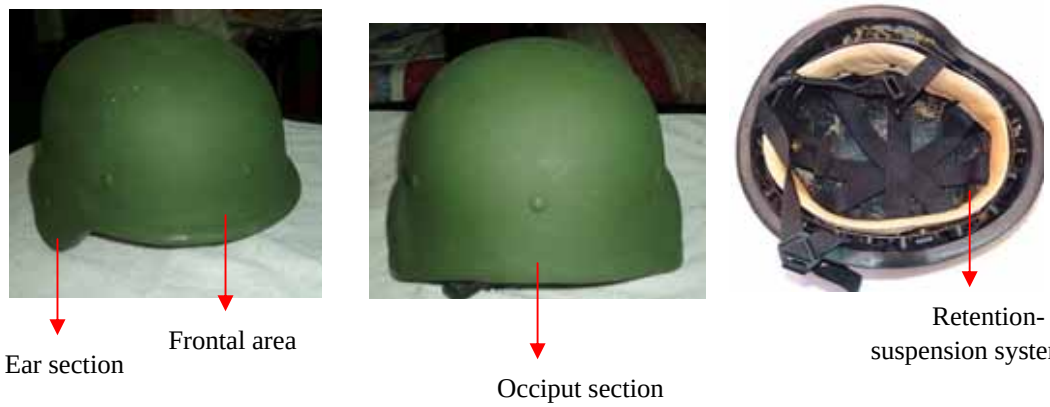

Figure 1.2: PASGT helmet

Furthermore, this helmet has been accepted and worn by the troop since the tentative data from the Persian Gulf War indicated that it reduced the incident of brain damage. Out of 24 soldiers who sustained head wounds, only three wounds involved the brain and all were from the projectiles that entered from area below the helmet (Carey et al., 2000).

Nowadays, composite materials used in ballistic helmet, for instance Kevlar that was used in PASGT, have produced a better helmet compared to traditional steel helmet in terms of its reduction in weight and an increase in ballistic resistance (van Hoof et al., 2001). However, the response of composite materials is very difficult to analyse due to its orthotropic properties, various failure modes involved and uncertainties on constitutive laws. The problem becomes more complex if it involves high velocity impact with a great deal of parameters that would affect the performance such as velocity of projectile, shape of projectile, geometry and boundary conditions, material characteristic and time-dependant surface of contact. (Silva et al., 2005).

Nevertheless, it is important to ensure that the ballistic helmet is able to stop the projectile from penetrating the helmet in order to prevent head injury to the wearer. Even though the projectile can be prevented to completely perforate the helmet, the deformation occurs inside the helmet may lead to serious head injury as well. Ballistic limit is one of the criteria used to evaluate the performance of the helmet. It is defined as the minimum initial velocity of the projectile that will result in complete penetration. At that impact velocity, the residual or exit velocity of the projectile is zero (Abrate, 1998).

As initial velocity of projectile is above the ballistic limit, the residual velocity becomes of interest since it can pose threat to the wearer. Therefore, it is vital to have better understanding on the response of ballistic helmet when struck by projectile at that impact velocity limit before one could design a better helmet.

On the other hand, finite element analysis has become a powerful tool for the numerical solution of a wide range of engineering problems. Complex problems can be modelled with relative ease with the advances in computer technology and CAD systems. Several computer programmes are available that facilitate the use of finite element analysis techniques. These programmes that provide streamlined procedures for prescribing nodal point locations, element types and locations, boundary constraints, steady and/or time-dependent load distributions, are based on finite element analysis procedures (Frank and Walter., 1989).

Finite element analysis is based on the method of domain and boundary discretisation which reduces the infinite number of unknowns defined at element nodes. It has two primary subdivisions. The first utilises discrete element to obtain the joint displacements and member forces of a structural framework. The second uses the continuum elements to obtain approximate solutions to heat transfer, fluid mechanics and solid mechanics problems (Portela and Charafi, 2002).

The response of composite materials during ballistic impact can also be determined by using finite element analysis apart from experimental testing. Although this method has become a popular trend in characterising composite materials, it must be used with a precaution and be always validated by experimental

work. It is also doubtful that experimental testing can be replaced totally by finite element analysis; rather it is probably a compliment to each other.

1.1 Problem Identification

In general, there are two ballistic test standards utilised to determine the quality of protection of the helmet; (1) NIJ-STD-0106.01 Type II and (2) MIL-H-44099A (Tham et al., 2008). Nevertheless, different helmet manufacturers may have different ballistic test methods. Having said that, the complex response of composite materials coupled with high costs and limited amount of data from ballistic testing has lead to experimental characterisation of ballistic helmet becomes expensive and time consuming (van Hoof et al., 2001). In order to address this issue, finite element analysis can be used as a method to characterise the response of composite ballistic helmet and to obtain valuable information on parameters affecting impact phenomena.

1.2 Scope of Research

The type of ballistic helmet investigated was PASGT (Personnel Armour System Ground Troops) whereas the bullet was 9mm parabellum bullet. Meanwhile, finite element analysis software used in this study was ABAQUS/Explicit. In material modelling, composite material was modelled as an orthotropic material. However, failure criterion was not included due to limitation of the software. In addition, no ballistic experiment was carried out in this study. Therefore, the validation of finite element modelling was based on the published result. Apart from that, this research emphasises on the structural integrity of the ballistic helmet when

impacted at high velocity. Hence, biomechanical aspect of the helmet is not within the scope of the research.

1.3 Objective of Research

The main focus of this research is to study the response of ballistic helmet made of composite materials when impacted at high velocity by using finite element analysis. The objective of this research are:

i) To determine the effect of modulus of elasticity and shear modulus of composite materials on ballistic resistance.

ii) To determine ballistic limit of the helmet made of four different types of composites namely Carbon fibre-reinforced Polyester, Glass fibre-reinforced Polyester, Kevlar fibre-reinforced and Kevlar 29 fibre-reinforced Phenolic.

iii) To analyse the deformation as well as energy distribution of the helmet when struck by a bullet at velocity of 360m/s.

iv) To evaluate the failure mechanism occurred on ballistic helmet after the impact.

1.4 Thesis Outline

This thesis comprises of five chapters. In Chapter One, it outlines the background and the general idea of the research. It includes the problem identification, scope of research as well as the objectives of the research. Literature review from previous study related to this research is discussed in Chapter Two. Some of the area discussed in this chapter are ballistic helmet and its design,

penetration mechanism of composite materials, numerical modelling of ballistic impact and parameters affecting ballistic impact performance. Chapter Three deals with methodology of the research such as software used in this research, finite element modelling and verification method. Results from simulation are discussed in Chapter Four whereas conclusion is covered in Chapter Five.

CHAPTER 2
LITERATURE REVIEW

2.0 Introduction

The definition of ballistic impact can be found in a few literatures. It is called ballistic impact for an impact resulting in complete penetration of the laminate while non-penetrating impact referred as low velocity impact. Other than that, stress wave propagation has no effect through the thickness of the laminate for the case of low velocity impact. As projectile contacts the target, compressive and shear waves propagate outward the impact point and reach the back face. Then, it reflects back. After several reflections through the thickness of the laminate, the plate motion is generated. Damage established after plate movement is called low velocity impact (Abrate, 1998).

An impact phenomenon is considered as low velocity impact if the contact period of the impactor is longer than the time period of the lowest mode of vibration of the structure. Apart from that, the support condition is critical since the stress waves generated during the impact will have enough time to reach the edges of the structure and causing full vibrational response. Conversely, ballistic impact or high velocity impact is involved with smaller contact period of the impactor on the structure than the time period of the lowest vibrational mode. The response of the structure is localised on the impacted area and it is usually not dependent on the support conditions (Naik and Shrirao, 2004).

However, there is also a threshold velocity which distinguishes low and high velocity impact. As implied by Cartič and Irving (2002), 20 m/s is a transition

velocity between two different types of impact damage and it allows a definition of high and low velocity impacts. Similarly, the transition to a stress wave-dominated impact arises at impact velocities between 10 and 20 m/s especially for general epoxy matrix composites (Abrate, 1998).

2.1 Constitutive Modelling

2.1.1 Composite Materials

Most of composite materials are anisotropic and heterogeneous. These two characteristics applied to the composite materials since the material properties are different in all directions and locations in the body. It differs from any common isotropic material, for example, steel which has identical material properties in any direction and location in the body. Hence, the difficulty in analysing the stress-strain relationship of composite materials becomes greater. However, it is still acceptable assuming that the stress-strain relationship of composite material behaves linearly and elastically and follows Hooke's law. The relationship for three dimensional body in a 1-2-3 orthogonal Cartesian coordinate system is given as follows (Kaw, 2006):

$$[\sigma] = [C][\varepsilon]$$

$$\begin{bmatrix} \sigma_1 \\ \sigma_2 \\ \sigma_3 \\ \tau_{23} \\ \tau_{31} \\ \tau_{12} \end{bmatrix} = \begin{bmatrix} C_{11} & C_{12} & C_{13} & C_{14} & C_{15} & C_{16} \\ C_{21} & C_{22} & C_{23} & C_{24} & C_{25} & C_{26} \\ C_{31} & C_{32} & C_{33} & C_{34} & C_{35} & C_{36} \\ C_{41} & C_{42} & C_{43} & C_{44} & C_{45} & C_{46} \\ C_{51} & C_{52} & C_{53} & C_{54} & C_{55} & C_{56} \\ C_{61} & C_{62} & C_{63} & C_{64} & C_{65} & C_{66} \end{bmatrix} \begin{bmatrix} \varepsilon_1 \\ \varepsilon_2 \\ \varepsilon_3 \\ \gamma_{23} \\ \gamma_{31} \\ \gamma_{12} \end{bmatrix} \quad (2.1)$$

This 6 x 6 [C] matrix is called stiffness matrix and it has 36 constants. However, due to symmetry of stiffness matrix, the constants can be reduced to 21 constants. It can be shown as follows. The stress-strain relationship can also be formulated as:

$$\sigma_i = \sum_{j=1}^{6} \boldsymbol{C}_{ij}\varepsilon_j \quad , \qquad i = 1\ldots6 \tag{2.2}$$

The strain energy in the body per unit volume is taken as:

$$\boldsymbol{W} = \frac{1}{2}\sum_{i=1}^{6} \sigma_i\varepsilon_i \quad , \qquad i = 1\ldots6 \tag{2.3}$$

Then, by substituting equation (2.2) in equation (2.3), it yields:

$$\boldsymbol{W} = \frac{1}{2}\sum_{i=1}^{6}\sum_{j=1}^{6} \boldsymbol{C}_{ij}\varepsilon_j\varepsilon_i \tag{2.4}$$

By partial differentiation of equation (2.4), it gives:

$$\frac{\partial \boldsymbol{W}}{\partial\varepsilon_i\partial\varepsilon_j} = \boldsymbol{C}_{ij} \tag{2.5}$$

and

$$\frac{\partial \boldsymbol{W}}{\partial\varepsilon_j\partial\varepsilon_i} = \boldsymbol{C}_{ji} \tag{2.6}$$

Since the differentiation is not necessarily to be in either sequent, thus:

$$\boldsymbol{C}_{ij} = \boldsymbol{C}_{ji} \tag{2.7}$$

Therefore, the stiffness matrix [C] is only left 21 elastic constants instead of 36.

$$\begin{bmatrix} \sigma_1 \\ \sigma_2 \\ \sigma_3 \\ \tau_{23} \\ \tau_{31} \\ \tau_{12} \end{bmatrix} = \begin{bmatrix} C_{11} & C_{12} & C_{13} & C_{14} & C_{15} & C_{16} \\ & C_{22} & C_{23} & C_{24} & C_{25} & C_{26} \\ & & C_{33} & C_{34} & C_{35} & C_{36} \\ & sym & & C_{44} & C_{45} & C_{46} \\ & & & & C_{55} & C_{56} \\ & & & & & C_{66} \end{bmatrix} \begin{bmatrix} \varepsilon_1 \\ \varepsilon_2 \\ \varepsilon_3 \\ \gamma_{23} \\ \gamma_{31} \\ \gamma_{12} \end{bmatrix} \quad (2.8)$$

As mentioned earlier, composite materials is an anisotropic material. Thus, in order to determine its stress-strain relationship, all 21 constants must be obtained. Nonetheless, many composite materials possess material symmetry. Material symmetry is defined as the material and its mirror image about the plane of symmetry are identical. In that case, the elastic properties are similar in directions of symmetry due to symmetry is present in the internal structure of the material. Consequently, this symmetry leads to reducing the number of the independent elastic constants by zeroing out or relating some of the constants within the 6 x 6 stiffness matrix. Thus, the stress-strain relationship will be simplified according to the types of elastic symmetry.

2.1.1.1 Orthotropic Material

A material is considered as an orthotropic material if there are three mutually perpendicular directions and has only three mutually perpendicular planes of material symmetry (Datoo, 1991). Generally, composite materials are considered as an orthotropic material since there are three mutually perpendicular planes of material property symmetry at a point in the body. The directions orthogonal to the three

planes of material symmetry in an orthotropic material define the principal material directions (Grujicic et al., 2006). It has been illustrated in Figure 2.1;

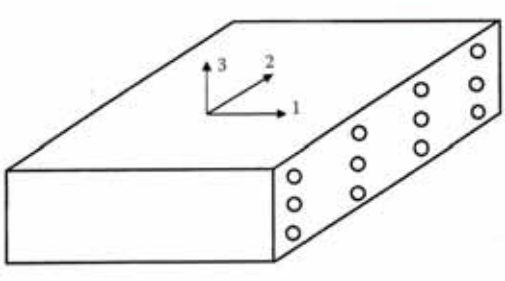

Figure 2.1: Principal material directions in an orthotropic material (Kaw, 2006).

As composite materials are considered as orthotropic material, the stiffness matrix is given by (Kaw, 2006);

$$[C] = \begin{bmatrix} C_{11} & C_{12} & C_{13} & 0 & 0 & 0 \\ C_{21} & C_{22} & C_{23} & 0 & 0 & 0 \\ C_{13} & C_{23} & C_{33} & 0 & 0 & 0 \\ 0 & 0 & 0 & C_{44} & 0 & 0 \\ 0 & 0 & 0 & 0 & C_{55} & 0 \\ 0 & 0 & 0 & 0 & 0 & C_{66} \end{bmatrix} \tag{2.9}$$

Therefore, it can be shown that only 9 elastic constants need to be solved in order to determine the stress-strain relationship of composite materials. It is expressed as;

$$\begin{bmatrix} \sigma_1 \\ \sigma_2 \\ \sigma_3 \\ \tau_{23} \\ \tau_{31} \\ \tau_{12} \end{bmatrix} = \begin{bmatrix} C_{11} & C_{12} & C_{13} & 0 & 0 & 0 \\ C_{21} & C_{22} & C_{23} & 0 & 0 & 0 \\ C_{13} & C_{23} & C_{33} & 0 & 0 & 0 \\ 0 & 0 & 0 & C_{44} & 0 & 0 \\ 0 & 0 & 0 & 0 & C_{55} & 0 \\ 0 & 0 & 0 & 0 & 0 & C_{66} \end{bmatrix} \begin{bmatrix} \varepsilon_1 \\ \varepsilon_2 \\ \varepsilon_3 \\ \gamma_{23} \\ \gamma_{31} \\ \gamma_{12} \end{bmatrix} \tag{2.10}$$

By substituting the stiffness matrix [C] with engineering constants,

$$[C] = \begin{bmatrix} \frac{1-\nu_{23}\nu_{32}}{E_2E_3\Delta} & \frac{\nu_{21}+\nu_{23}\nu_{31}}{E_2E_3\Delta} & \frac{\nu_{31}+\nu_{21}\nu_{32}}{E_2E_3\Delta} & 0 & 0 & 0 \\ \frac{\nu_{21}+\nu_{23}\nu_{31}}{E_2E_3\Delta} & \frac{1-\nu_{13}\nu_{31}}{E_1E_3\Delta} & \frac{\nu_{32}+\nu_{12}\nu_{31}}{E_1E_3\Delta} & 0 & 0 & 0 \\ \frac{\nu_{31}+\nu_{21}\nu_{32}}{E_2E_3\Delta} & \frac{\nu_{32}+\nu_{12}\nu_{31}}{E_1E_3\Delta} & \frac{1-\nu_{12}\nu_{21}}{E_1E_2\Delta} & 0 & 0 & 0 \\ 0 & 0 & 0 & G_{23} & 0 & 0 \\ 0 & 0 & 0 & 0 & G_{31} & 0 \\ 0 & 0 & 0 & 0 & 0 & G_{12} \end{bmatrix} \quad (2.11)$$

where

$$\Delta = \frac{1-\nu_{12}\nu_{21}-\nu_{23}\nu_{32}-\nu_{13}\nu_{31}-2\nu_{21}\nu_{32}\nu_{13}}{E_1E_2E_3} \quad (2.12)$$

Since the symmetrical properties exist in the stiffness matrix, the relation between Poisson's ratio and Young's Modulus is,

$$\frac{\nu_{ij}}{E_i} = \frac{\nu_{ji}}{E_j} \quad \text{for } i \neq j \text{ and } i, j = 1,2,3 \quad (2.13)$$

However, there are restrictions on elastic modulus in which, based on first thermodynamics law, the stiffness matrices must be positive definite. In terms of inequalities, it is written as:

$$|\nu_{12}| < \sqrt{\frac{E_1}{E_2}}, \quad |\nu_{21}| < \sqrt{\frac{E_2}{E_1}}, \quad |\nu_{32}| < \sqrt{\frac{E_3}{E_2}},$$
$$|\nu_{23}| < \sqrt{\frac{E_2}{E_3}}, \quad |\nu_{31}| < \sqrt{\frac{E_3}{E_1}}, \quad |\nu_{13}| < \sqrt{\frac{E_1}{E_3}} \quad (2.14)$$

Relation in (2.11) and (2.12) was implemented in ABAQUS/Explicit to define the composite materials as an orthotropic material. The inequalities in (2.14) was followed strictly to ensure the stiffness matrices must be positive definite the stiffness matrices must be positive definite.

2.1.2 Impact Dynamics

2.1.2.1 Fundamental Principle.

In general, there are three fundamental principles used in analysing impact events either concerning stress wave propagation, ballistics modelling or numerical simulation. Those conservation laws are conservation of mass, conservation of momentum and conservation of energy (Nicholas and Recht, 1992).

1. Conservation of Mass

In a physical system, the conservation of mass is given by:

$$\int_V \rho dV = const \tag{2.15}$$

where ρ is the mass density and V is the volume of the body.

2. Conservation of Momentum

Based on Newton's second law:

$$F = m\frac{d\upsilon}{dt} \tag{2.16}$$

For a closed system of n masses, $m_{i,}$ and no external forces acted on the system, conservation of momentum is expressed as:

$$\sum_{i=1}^{n} m_i \upsilon_i = const \tag{2.17}$$

The equation (2.16) is multiplied by *dt* and integrating it, thus, the impulse-momentum law is given as:

$$\boldsymbol{I} = \int \boldsymbol{F}dt = \int \boldsymbol{m}d\upsilon = \boldsymbol{m}\upsilon_f - \boldsymbol{m}\upsilon_i \tag{2.18}$$

This law implies that the impulse $\boldsymbol{I}$ acted to a body changes the momentum from an initial value $\boldsymbol{m}\upsilon_i$ to a final value $\boldsymbol{m}\upsilon_f$ where $\boldsymbol{v}$ is the velocity.

3. Conservation of Energy

The conservation of energy is expressed in a form where system being considered is a set of *j* discrete masses or volumes. At the initial state *i* at time $t = 0$ and the final state *f* some time later, the energy is conserved, i.e:

$$\sum_j \boldsymbol{E}_i + \sum_j \frac{1}{2}\rho\upsilon_i^2 = \sum_j \boldsymbol{E}_f + \sum_j \frac{1}{2}\rho\upsilon_f^2 + \boldsymbol{W} \tag{2.19}$$

where E is the stored (elastic) internal energy and $\boldsymbol{W}$ represents work done on the system.

These relationships (2.14 – 2.18) are a fundamental concept in impact phenomenon that will be used in ABAQUS/Explicit as an input parameter, for instance, value of bullet's mass and density of the material.

2.2 Penetration Mechanism of Composite Materials

In general, punching failure, fibre failure, matrix cracking and delamination are considered as main damage mechanism occurred in composite materials during ballistic impact. There were researchers who had proposed that these damage mechanisms occurred in sequential order. Figure 2.2 shows damage mechanisms that

have been observed during the impact process. It starts with punching failure and followed by fibre breakage before delamination occurred at the back face of the laminate. The relative thickness of each damage process depends on overall laminate thickness (van Hoof, 1999).

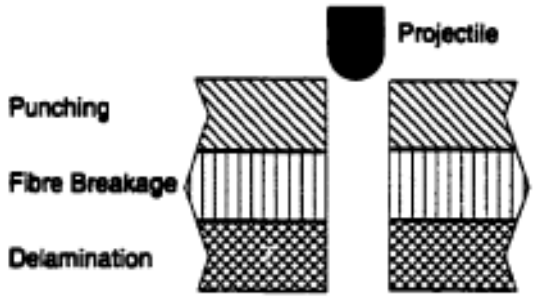

Figure 2.2: Penetration damage mechanisms in chronological order occurred during penetration process (van Hoof, 1999).

At the early phase of ballistic impact, the laminate material is being compressed underneath the projectile and through thickness shear deformation occurs at the crater wall (van Hoof, 1999). As the top layers get compressed, cone formation is developed on the back face of the target. The formation is referred to as conical deformation towards back face of the target plate. The top layers of the laminate are being compressed when the cone is formed. It causes the strain in the top layers to be more than the bottom layers (Naik et al., 2006). Figure 2.3 illustrates the formation of the cone. The through thickness compression will result in material crushing while through thickness shear deformation can result in plug formation. Fibre breakage occurs when the advancing projectile forces the fibres to extend beyond their tensile failure. Failure of all fibres shows that complete perforation of projectile into the target. Nonetheless, before fibre breakage takes place, the damage would be the combined of matrix cracking and delamination.

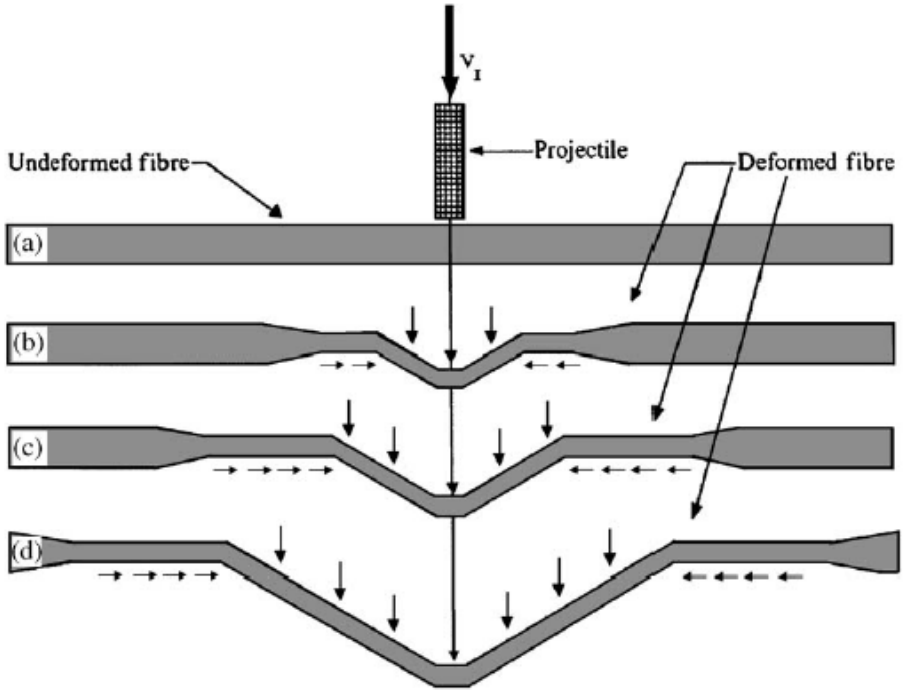

Figure 2.3: Conical formation at the back of the panel (Naik et al., 2006).

As the projectile advances through the target, the projectile deforms the target both laterally as well as downward. The in-plane compression will result in interlaminar shear stresses whereas out-of-plane compression will lead to interlaminar normal stresses. Both types of stresses will cause a delamination growth. As the projectile penetrates the target, the material ahead of projectile becomes thinner, thus will lead to smaller resistance to deflection. Therefore, the advance projectile will experience a decreasing resistance to separating the non-perforated ply from the remainder plies resulting in an increase in the extent of delaminations at the back face of the laminate (van Hoof, 1999). Figure 2.4 shows the damage mechanisms occurred during ballistic impact.

Figure 2.4: Damage mechanisms occurred in composite materials under ballistic impact (van Hoof, 1999).

In the event of perforated GRP (glass reinforce polymer) plate, shearing and fragmentation have been identified as significant phenomena in the initial stages of perforation. The cone of damage on the impact side of a thick target is a result of compression of material ahead of projectile. This leads to radial stress due to displacement of fragmented material. As the projectile proceeds to the exit side of the target, it is easier for layers to delaminate and bend away from the striking projectile in the direction of projectile motion. Dishing occurs and forms the cone of the damage opening towards the exit side of the target. Thick composites will be penetrated by the indentation mechanism until fracture of the matrix phase at the ply interfaces can be achieved, which then allows the dishing mechanism to develop at the rear of such targets. The perforation mechanism of thin composite however is dominated by dishing mechanism rather than indentation and compression. (Gellert et al., 2000).

Similar observation has been made by other researchers when a conical-shaped perforation zone is created during perforation of thin composite laminates whereas for thicker targets, two distinct failure processes are observed for the upper and lower portions of the specimens (Abrate, 1998). Figure 2.5 illustrates the damage characteristics for both thin and thick composite laminates.

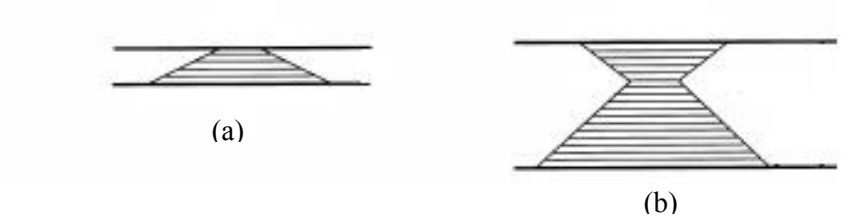

Figure 2.5: Damage characteristic of (a) thin target and (b) thick target. Impact face is the upper edge (Gellert et al., 2000).

2.3 Energy Absorption Mechanism of Composite Materials

Impact loads can be categorised into three categories which is low-velocity impact, high-velocity impact and hyper-velocity impact. This classification is made because of change in projectile's velocity will result in different mechanisms in terms of energy transfer between projectile and target, energy dissipation and damage propagation mechanism (Naik and Shrirao, 2004).

Basically, ballistic impact is considered as low-mass high velocity impact. In this impact event, a low-mass projectile is launched by source into target at high velocity. It is unlike low-velocity impact that involved high-mass impactor impacting a target at low velocity. In view of the fact that ballistic impact is high velocity event, the effect is localised and near to impact location.

According to Naik et al. (2006), seven possible energy absorbing mechanisms occur at the target during ballistic impact. Those mechanisms are cone formation at the back face of the target, deformation of secondary yarns, tension in primary yarns/fibres, delamination, matrix cracking, shear plugging and friction between the projectile and the target. Then, the researchers formulated all these energies into equation whereby the total energy absorbed by the target is summation of kinetic energy of moving cone E_{KE}, shear plugging E_{SP}, deformation of secondary yarns E_D, tensile failure of primary yarns E_{TF}, delamination E_{DL}, matrix cracking E_{MC} and friction energy E_F.

$$E_{TOTALi} = E_{KEi} + E_{SPi} + E_{Di} + E_{TFi} + E_{DLi} + E_{MCi} + E_{Fi} \quad (2.20)$$

Mines et al. (1999) identified three modes of energy absorption when analysed the ballistic perforation of composites with different shape of projectile. These energy absorptions are local perforation, delamination and friction between the missile and the target. However, the contribution of friction between the missile and the target in energy absorption is low compared to the other two. In terms of local perforation, three through-thickness regimes can be identified, namely: I - shear failure, II - tensile failure and III - tensile failure and delamination. Out of these three regimes, the through-thickness perforation failure is dominated by shear failure. Similar observation has been made by other researcher for thick graphite epoxy laminates whereby the perforation failure is dominated by shear failure. The third main energy absorption mechanism is delamination. Delamination can propagate under Mode I (tensile) and Mode II (shear) loading and each mode can dominate each other depending on structural configuration of the composite as well as material properties. Therefore, it can be predicted that the total perforation energy is a summation of energy absorption due to local perforation, delamination and friction between the missile and the target.

$$E_{\text{pred}} = E_{\text{f}} + E_{\text{sh}} + E_{\text{dl}} \tag{2.21}$$

where E_{f} = friction between the missile and the target; E_{sh} = local perforation; E_{dl} = delamination

Apart from that, Morye et al. (2000) has studied energy absorption mechanism in thermoplastic fibre reinforced composites through experimental and analytical prediction. They considered three mechanisms that involved in absorbing energy by composite materials upon ballistic impact. The three energy absorption mechanisms are tensile failure of primary yarns, elastic deformation of secondary

yarns and the third mechanism is kinetic energy of cone formed at back face of composite materials. They concluded that kinetic energy of the moving cone had a dominant effect as energy absorption mechanism for composite materials. Nevertheless, they neglected a delamination as one of the factor contributed to the failure of composite materials during ballistic impact.

2.4 Numerical Modelling of Ballistic Impact

Damage mechanism of composite materials during ballistic impact can also be determined by using numerical simulation apart from experimental testing. Although this method has become a popular trend in characterising composite materials, it must be used with a precaution and be always validated by experimental work. It is also doubtful that experimental testing can be replaced totally by numerical simulation; rather it is probably a compliment to each other.

In study carried out by Silva et al. (2005), the researchers used AUTODYN to investigate the ballistic limit and damage characteristic of Kevlar 29/Vynilester panel. They argued that the ability of numerical model used to predict ballistic impact response of composite material depended largely on choice of appropriate material model. In the material model, it assumes that the composite material behaves as an orthotropic material system and non-linear shock effects and associated energy dependency result from volumetric material strain. Deviatoric strain contributions to the final material pressure are based on linear material response. The model also includes orthotropic brittle failure criteria to detect directional failure such as delamination. Failure occurs in brittle manner and is instantaneous in the specified failure direction. Post-failure material stiffness

coefficients are assumed equal to those for the intact in direction orthogonal to the failed directions. It was found that the ballistic limit of Kevlar 29/Vynilester was correlated very well between experiment and simulation with 324.3 m/s and 320 m/s respectively. The damage mechanism involved was initially started with matrix cracking, followed by delamination and fibre breakage in the last stage. The delamination formed a circular shape when observed both experimentally and numerically.

Other approach that has been used by the researchers in simulating damage characteristic of composite laminate during impact is based on so-called continuum damage mechanics (CDM) constitutive model. This approach has been successfully implemented within LS-DYNA 3D and LS-DYNA 2D by van Hoof et al. (2001) and Nandlall et al. (1998) respectively. As the previous approach used by Silva et al. (2005), they are assumed that the response of an individual lamina is linear elastic up to failure and that in the post-failure regime a lamina is idealised in brittle manner with the dominant stiffness and strength components reduced to zero instantaneously. It is however not the case since the post-failure response of the material is able to significantly absorb the impact energy.

In the CDM model, Nandlall et al. (1998) has implemented two-dimensional axisymmetric code in LS-DYNA 2D that determines through-thickness damage modes for thick composite laminates. This approach accounts for through-thickness stresses namely normal and shear stress which can be used to predict localised damage. However, it neglects the in-plane properties. As for Hoof et al. (2001), they developed 3D laminate model that include both intralaminar failure (in-plane tensile

and penetration failure) and interlaminar failure or delamination. The intralaminar failure is implemented within user-defined material subroutine whereas interlaminar failure is modelled by using discrete interfaces allowing inter-ply cracking. In the results obtained, the numerical simulations exhibited a considerable degree of hourglassing and the stiffness hourglass control proved to be the most efficient way of controlling these hourglass modes. Besides that, numerical predictions also highly sensitive to the applied mesh definition. Increasing for both the in-plane and through-thickness mesh density resulted in substantial changes in the predicted response.

2.5 Parameters Affecting Ballistic Performance.

2.5.1 Material Properties

The influence of material properties is one of the key considerations in design of impact resistant composite structures. Some material properties of the composite materials affect the impact dynamics or the strength of the laminate. Properties of the matrix material, the reinforcement and the interface are considered as having a direct effect on impact resistance. For instance, fibre with high strain to failure, tougher resin systems, compliant layers between certain plies or woven or stitched laminate will result in improving the impact resistance of composite structures (Abrate, 1998).

Fibres which have high tensile strengths and strain to failure are able to absorb significant amount of energy. It has been found that fibre straining is a primary energy absorbing mechanism in penetration failure of impacted composite laminates. This phenomenon occurs at the impact velocity below and close to ballistic limit. Nevertheless, at impact velocity higher than ballistic limit, it reduces

fibre straining since no time is allowed for transverse deflection to propagate to the edges. Thus, the energy absorbed is much smaller.

Apart from that, high elastic modulus and low density that lead to high wave velocity will help the strained fibres to propagate more quickly from the impact point, hence the energy is distributed to a wider area and prevent from a large strains developed at the impacted area. (Cheeseman and Bogetti, 2003).

Carbon fibre reinforced epoxy, for instance, has a different material properties compared to Kevlar fibre reinforced epoxy even though the resin is the same. Kevlar/epoxy has a lower density but higher strain to failure and a higher tensile strength. With these two different material systems, it will lead to different ballistic response when impacted with the projectiles. Goldsmith et al. (1995) observed that Kevlar was greater than Carbon in stopping sharp-pointed projectiles and hence absorbing more energy over the entire range of plate thicknesses investigated. The failures characteristics are also differ between these two materials. Carbon showed no delamination beyond the immediate vicinity of the cracked region whereas Kevlar demonstrated a separation of plies up to a distance four times greater than diameter of penetrator and it is mainly due to fibre stretching. In addition, the graphite exhibited petaling instead of bulging in the contact area.

Petaling, as showed in Figure 2.6, is produced by high radial and circumferential tensile stresses after passage of the initial stress wave. The intense-stress fields occur near the tip of the projectile. Bending moments created by the forward motion of the plate material pushed by the striker cause the characteristic